applied sciences

MDPI

Article

Comparative Analysis of the Irradiation with Medium Fluences of High-Energy Electrons and Pr Doping on the Fluctuation Conductivity of $YBa_2Cu_3O_{7-\delta}$ Single Crystals

George Khadzhai [1], Ioannis Goulatis [2], Alexander Chroneos [2,3,*], Alexander Feher [4] and Ruslan Vovk [1,5]

1 V.N. Karazin Kharkiv National University, Svoboda Sq. 4, 61022 Kharkiv, Ukraine; gkhadjai@gmail.com (G.K.); rvvovk2017@gmail.com (R.V.)
2 Department of Electrical and Computer Engineering, University of Thessaly, 38334 Volos, Greece; yannislgoul@gmail.com
3 Department of Materials, Imperial College London, London SW7 2BP, UK
4 Centre of Low Temperature Physics, Faculty of Science, P.J. Safarik University, Park Angelinum 9, 041 54 Kosice, Slovakia; alexander.feher@upjs.sk
5 The Department of Mathematics and Physics, Ukrainian State University of Railway Transport, Feierbakh Sq. 7, 61050 Kharkiv, Ukraine
* Correspondence: alexander.chroneos@imperial.ac.uk; Tel.: +30-6978775320

Abstract: Medium-fluence fast electron irradiation (10^{19} e/cm^2 to 10^{20} e/cm^2) or the changes in the praseodymium concentration in the range of $0.0 \leq z \leq 0.5$ on the excess conductivity of $YBa_2Cu_3O_{7-\delta}$ single crystals ware investigated. These can lead to a wider range of the temperature interval of excess conductivity which narrows the interval of linearity in the ab plane. At fluences $0 \leq \Phi \leq 6.5 \times 10^{19}$ e/cm^2, there was a threefold increase in the transverse coherence length $\xi_c(0)$ with an increase in Φ of more than four times as the praseodymium concentration increased to $z \approx 0.42$. The two-dimensional–three-dimensional (2*D*–3*D*) crossover point shifted upward in temperature. Conversely, to irradiation with low fluences ($\Phi \leq 10^{19}$ e/cm^2) or low praseodymium doping ($z \leq 0.39$), irradiation with medium fluences or high praseodymium doping led to a non-monotonic dependence of $\xi_c(0)$ on the irradiation fluence, with characteristic maxima at Φ~(7–8) $\times 10^{19}$ e/cm^2 and $z \approx 0.42$, likely due to the suppression of the superconducting characteristics.

Keywords: $YBa_2Cu_3O_{7-\delta}$; fast electrons; excess conductivity; single crystals; electron irradiation

Citation: Khadzhai, G.; Goulatis, I.; Chroneos, A.; Feher, A.; Vovk, R. Comparative Analysis of the Irradiation with Medium Fluences of High-Energy Electrons and Pr Doping on the Fluctuation Conductivity of $YBa_2Cu_3O_{7-\delta}$ Single Crystals. *Appl. Sci.* **2024**, *14*, 6536. https://doi.org/10.3390/app14156536

Academic Editors: Gerard Ghibaudo and Roberto Zivieri

Received: 5 June 2024
Revised: 10 July 2024
Accepted: 21 July 2024
Published: 26 July 2024

1. Introduction

The data obtained during the investigation of the impact of high-energy electron irradiation or praseodymium doping on the magnetoresistive characteristics of high-temperature superconducting cuprates (HTSCs) are important experimental material, the processing of which makes it possible to achieve success in determining the microscopic mechanism of superconductivity and improving the functional characteristics of existing HTSC compounds [1–19]. Superconducting, high-temperature, single crystals are the technological basis of fundamental research aimed at establishing the mechanisms regarding the interaction of layered structures with radiation [16,17,20].

Irradiation with high-energy electrons makes it possible to create radiation defects while at the same time retaining the composition of the material. These defects change the electrical resistance in both normal and superconducting states [16–20]. Doping with praseodymium also has a similar effect on the resistance of $YBa_2Cu_3O_{7-\delta}$, which creates impurity defects [6,10,18,19,21–23] without changing the content of labile oxygen [24,25]. Comparing the resistance of electron-irradiated $YBa_2Cu_3O_{7-\delta}$ with the resistance of $Y_{1-z}Pr_zBa_2Cu_3O_{7-\delta}$ will allow us to better understand the difference in the ensemble of defects in both cases, especially in the region of the superconducting transition.

Considering the prospect of using high-temperature superconductors as supersensitive sensors and electric current transmission lines with low energy losses operating in the region of liquid nitrogen's boiling temperature, the creation of a so-called "controlled" defect structure [9,10,15] in a superconductor has important fundamental and practical significance.

Compounds of the $YBa_2Cu_3O_{7-\delta}$ system are among the most promising HTSC materials because of the following reasons: (a) these compounds have a fairly high superconducting transition temperature, Tc ≈ 90 K (higher than the boiling point of liquid nitrogen); (b) single-crystalline samples of these compounds are relatively easy to grow, and their physical properties can be varied quite easily by modifying the oxygen concentration; and (c) they hold technological importance so they need to be stable under extreme external influences.

The partial replacement of yttrium with praseodymium allows, unlike rare-earth elements, for a change in the Tc from the maximum value to 0 (antiferromagnetic insulator) while maintaining the degree of oxygen content at the optimal level (praseodymium anomaly). Thus, the application of electron irradiation or praseodymium doping makes it possible to tune the critical and electrical transport properties of $Y_{1-z}Pr_zBa_2Cu_3O_{7-\delta}$ single crystals in a wide range.

Note that, despite intensive experimental studies of the influence of various kinds of external influences on electric transport in the $YBa_2Cu_3O_{7-\delta}$ system [1–10,15–17,19–24], there is only a small amount of scientific work devoted to comparative studies of the influence of electron irradiation and Pr doping on the pseudogap and fluctuation conductivity anomalies. At the same time, according to contemporary ideas, it is these "unusual" physical phenomena observed in HTSC compounds in the non-superconducting state that are critical to understanding the microscopic nature of HTSC, which is presently not fully explained, in spite of more than three decades of systematical experimental work.

In previous studies [26], we studied the impact of relatively low irradiation fluences from 1.4 to 8.8 × 10^{18} e/cm^2, or of weak doping with praseodymium on the fluctuation conductivity (FC) and paraconductivity in $YBa_2Cu_3O_{7-\delta}$ single crystals with a stoichiometric composition. Here, we consider the effect of medium fluences (up to 100 × 10^{18} e/cm^2) of irradiation with high-energy electrons or the effect of praseodymium impurities in a significant concentration range ($0.0 \leq z \leq 0.5$) on the fluctuation conductivity in $Y_{1-z}Pr_zBa_2Cu_3O_{7-\delta}$ single crystals during the flow of a transport current in basic *ab*-plane.

2. Experimental Methods

The $YBa_2Cu_3O_{7-\delta}$ single crystals investigated in this study were grown by the melt solution method [1,3,5]. The crystals were subjected to an oxygen atmosphere at 430 °C for four days and this led to their saturation. The crystals contained twins, whose planes of which had a block structure. Resistivity measurements were taken with the standard 4-pin method. The measured crystal sizes were (1.5…2) × (0.2…0.3) × (0.01…0.02) mm^3, where the third dimension was the c axis. To prepare crystals with partial replacement of Y by Pr, $Y_{1-z}Pr_zBa_2Cu_3O_{7-\delta}$, Pr_5O_{11} was introduced to the initial mixture in the appropriate percentage.

The modes of growth and oxygen saturation of $Y_{1-z}Pr_zBa_2Cu_3O_{7-\delta}$ crystals were the same as for undoped single crystals [5,20]. Y_2O_3, $BaCO_3$, CuO and Pr_5O_{11} compounds were used in the crystal growth. A transport current of up to 10 mA passed through the largest sample size, where the typical distance of the potential contacts is 1 mm.

The grown single crystals exhibited characteristics of normal and superconducting states corresponding to a given oxygen and/or praseodymium content. The technological and experimental details for the synthesis of experimental samples, resistivity measurements and analysis of the transport properties were previously described [1,3,5,19,20].

Electron irradiation with energies in the range of 0.5 to 2.5 MeV was employed at temperatures below 10 K. The irradiation fluence Φ = 10^{18} e/cm^2 by electrons with an

energy of 2.5 MeV corresponded to a defect concentration averaged over all sublattices of 10^{-4} displacement per atom [26]. The measurement technique was the following: first, the temperature dependences of the resistivity of the sample were measured. The sample was then cooled to 5 K and irradiated with electrons. The beam intensity was chosen such that the temperature of the sample during irradiation did not exceed 10 K. After irradiation, the sample was heated to a temperature of 300 K and, gradually lowering the temperature, the resistivity of the sample was measured. The same sample was successively irradiated at different fluences. To measure electrical resistance after irradiation in the temperature range of 4.2 < T < 300 K, a specially designed helium cryostat was used. All electrical resistance measurements were carried out at a fixed temperature; temperature stability was about 5 mK. Temperature was measured with a platinum resistance thermometer.

3. Results and Discussion

In Figure 1a, the dependences $r_{ab}(T)$ obtained before and after irradiation with fast electrons at fluences from 0 (curve 1) to 86.3 × 10^{18} e/cm^2 (curve 8) are shown. These dependencies were analyzed in previous work [27]. The electrical resistivity of $Y_{1-z}Pr_zBa_2Cu_3O_{7-\delta}$ single crystals when the praseodymium content, z, changed from zero (curve 1) to z = 0.5 (curve 8) is shown in Figure 1b. As can be seen from Figure 1, in both cases, the curves are characterized by quasi-metallic behavior of electrical resistivity with a characteristic linear area of the dependence ρ(T) at high temperatures. Both at maximum irradiation fluences and at maximum Pr content, the ρ(T) curves acquired a characteristic S-shape, which indicates the appearance of a thermally activated region on the ρ(T) dependences, which will be discussed in more detail below.

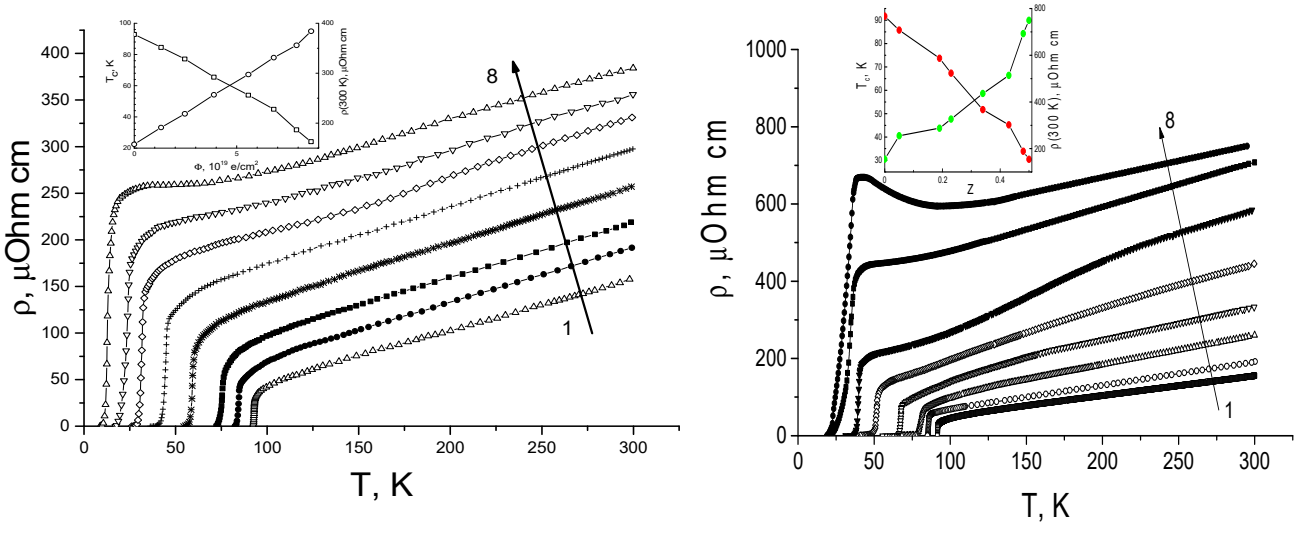

(**a**) (**b**)

Figure 1. (**a**). Temperature dependencies $\rho_{ab}(T)$ of $YBa_2Cu_3O_{7-\delta}$ single crystals prior to and after irradiation with electrons at fluences 0, 13.1, 24.7, 38.9, 55.7, 68.1, 79.2 and 86.3·10^{18} e/cm^2—curves 1–8, respectively. Inset: dependence of the critical temperature, Tc (squares), and electrical resistivity at room temperature, ρ(300 K) (circles), on fluence for all samples. (**b**). Temperature dependences r(T) of $Y_{1-z}Pr_zBa_2Cu_3O_{7-\delta}$ single crystals for z 0.0, 0.05, 0.19, 0.23, 0.34, 0.43, 0.48 and 0.50—curves 1–8, respectively. Inset: dependence of the critical temperature, Tc (red circles), and electrical resistivity at room temperature, ρ(300 K) (green circles), on the Pr concentration for all samples.

From Figure 1, it can be deduced that when the T dropped below T*, in the basal plane, on the $\rho_{ab}(T)$ dependencies in the region of relatively high temperatures, an extended linear section was preserved even at for high irradiation fluences. Numerous theoretical models have been introduced to explain these dependences including the resonating valence band theory (RVB theory) [28] and the nearly antiferromagnetic Fermi liquid (NAFL) model [29].

In the RVB theory, scattering in HTSC compounds occurs through the interaction of carriers (spinons and holons) [28]. Herewith, the T dependence of the electrical resistivity additionally to the linear T term introduces an additional term, proportional to 1/T [30], in both cases, as in longitudinal and as in transverse electrical resistivity:

$$\rho(\mathrm{T}) = \mathrm{AT}^{-1} + \mathrm{BT} \quad (1)$$

From Figure 2 (note: irradiation fluences up to $\leq 70 \times 10^{18}$ cm^{-2} or a low level of Pr doping, z < 0.25), it was observed that the dependences of the products ρ_{ab}(T)·T on T^2 become close to linear.

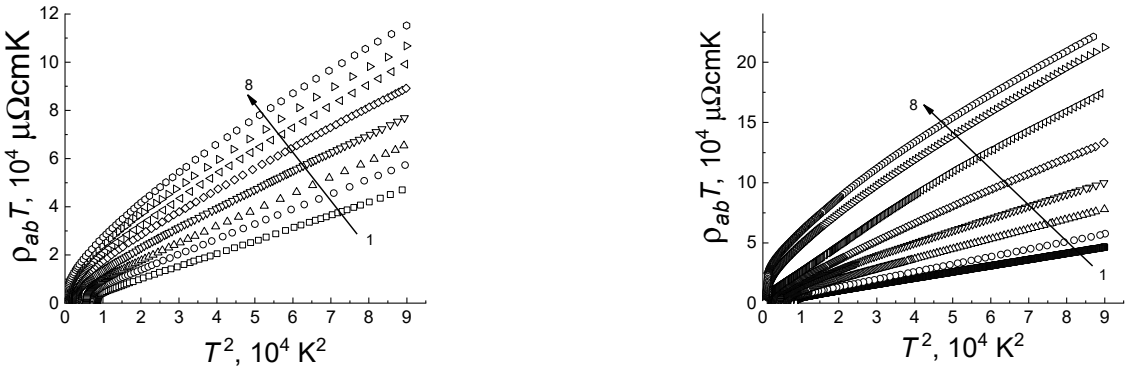

Figure 2. Temperature dependencies of electrical resistivity in ρ·T–T^2 coordinates in the ab-plane. The curves' numbering is consistent with Figure 1.

For medium and high fluences of $\Phi > 100 \times 10^{18}$ cm^{-2} or in the case of medium and heavily Pr-doped samples z ≥ 0.25, the experimental curves ρ_c(T) could not sufficiently be described by the dependence from Equation (1).

Figure 3 shows the dependencies of the linearity parameters A and B in Equation (1) from fluence (Φ) or praseodymium concentration (*z*).

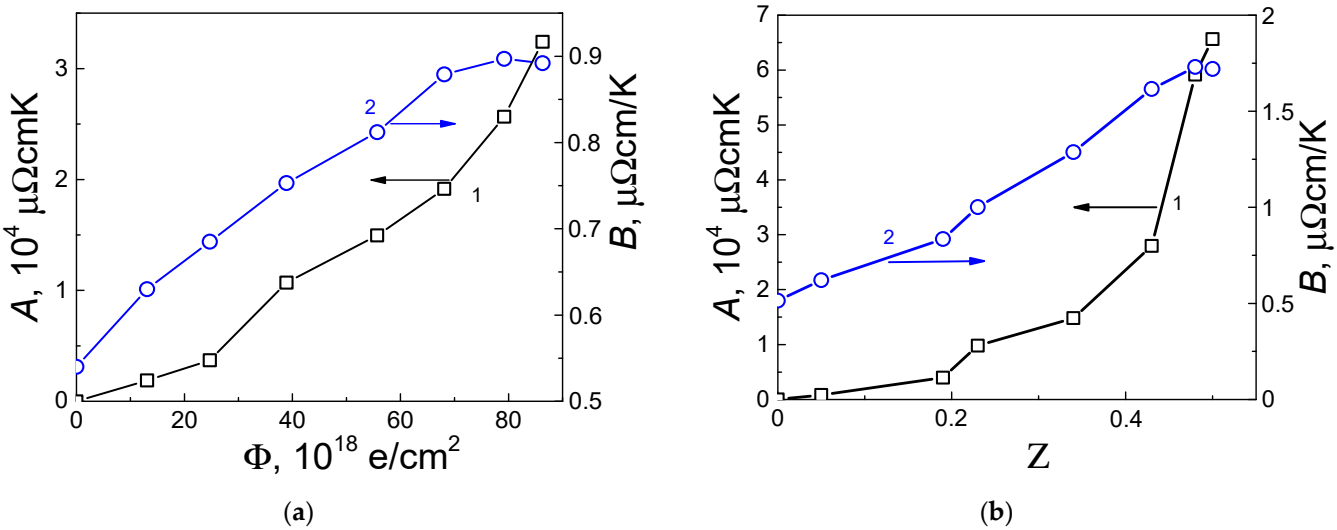

Figure 3. A and B linearity parameters [Equation (1)] dependencies from (**a**) fluence (Φ) and (**b**) praseodymium concentration (*z*).

As inferred from the figure, the linearity of the ρ(T)·T–T^2 dependence was directly related to the defectiveness of the structure of the experimental samples, since both the (linear) parameters increased rapidly by increasing Φ or *z*, i.e., by increasing the concentration of irradiation and impurity defects.

From Figure 4, it could be concluded that increasing Φ led to a rapid decrease in the interval of linearity or shift toward high temperatures (measurements were carried out up to 300 K); regarding the increase in *z*, the situation was even more diverse, and namely, for concentration number 8 (of the experimental measurements) there was no linearity (up to 300 K), and the derivative decreased by increasing the temperature. That is, there was a contradiction such that by (with) increasing defectiveness, the parameters of the linear dependence $\rho(T)\cdot T–T^2$ increased, but the linear dependence itself showed a tendency to disappear due to the narrowing of the interval of its existence.

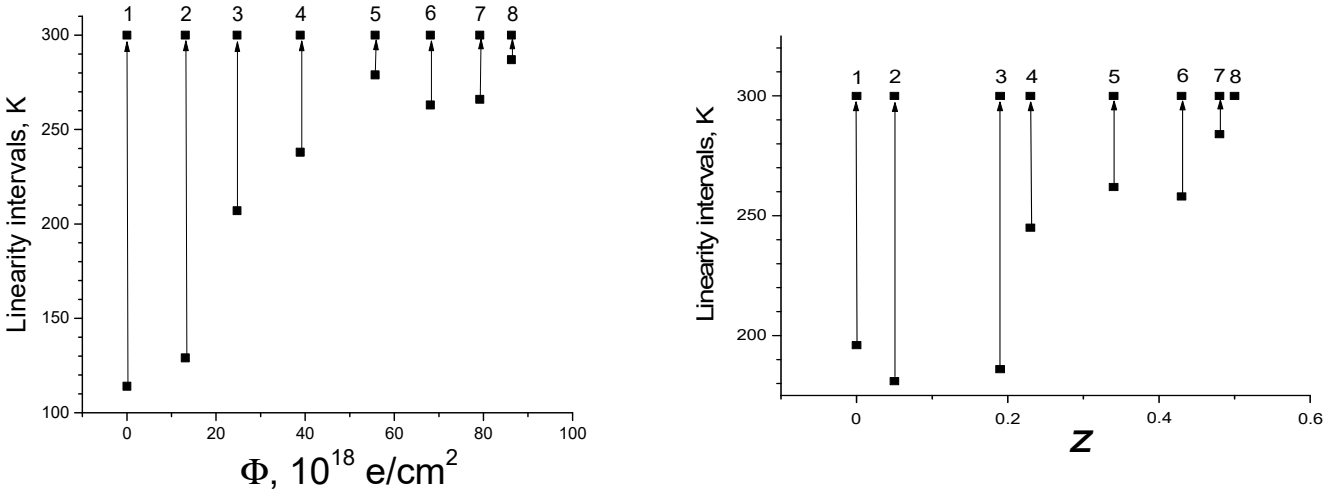

Figure 4. Interval of linearity as a function of Φ or z for the cases of irradiation with different fluences of electrons or changes in praseodymium concentration. Numbers 1−8 correspond to the numbers of the curves in Figure 1.

As noted above, there were noticeable differences in the evolution of resistivity curves under irradiation or doping with praseodymium. Figure 1 reveals that irradiation resulted in an anomalously strengthened (in comparison to the change in composition [1,16,22]) decrease in T_c in $YBa_2Cu_3O_{7-\delta}$. Nevertheless, the nature of the change in the electrical and superconducting properties of HTSC with a change in composition [1,22] and under the action of irradiation was somewhat different. The primary difference was for $Y_{1-z}Pr_zBa_2Cu_3O_{7-\delta}$ single crystals with $T_c < 85$ K, where as a rule, a change in the shape of the $\rho(T)$ curves was observed from metallic to the so-called "S-shaped" with a characteristic thermally activated deflection [1,17,18] ($z > 0.2$, Figure 1b); during irradiation, a similar "S-shaped" shape of the $\rho(T)$ curves was observed for $T_c < 35$ K ($\Phi > 60$ e/cm^2, Figure 1a).

A key reason for the strong decrease in T_c in irradiated samples was the appearance of dielectric inclusions under the influence of irradiation because of the redistribution of oxygen between the O(4) and O(5) positions and the formation of local regions with a tetragonal structure.

With increased fluence, the T_c decreased from~92 to~24 K, and ρ_{ab}(300 K) increased from ρ~158 to 384 μOhm·cm, respectively, which is consistent with previous studies [26,30]. Clearly similar effects were avoided when supplemented with praseodymium [1,18]. The dependencies of T_c and ρ(300 K) on Φ and *z* are shown in the insets in Figure 1a,b.

As shown from Figure 1, below, for the characteristic temperature *T**, the dependencies for all $\rho_{ab}(T)$ curves were "rounded off", which may have been caused by the emergence of excess conductivity $\Delta\sigma_{ab}$. Lawrence and Doniach [13] used the following relation for the fluctuation conductivity in the plane of layers in the immediate vicinity of the SC transition:

$$\Delta\sigma_{ab} = \frac{e^2}{16\hbar d}\frac{1}{\sqrt{[\varepsilon(\varepsilon + r)]}}, \quad (2)$$

where d = 11.7 Å and is the interlayer distance [31].

$$\varepsilon = \frac{T - Tc}{Tc} \ll 1;\ r = \frac{4\xi_c^2(0)}{d^2}. \quad (3)$$

Equation (1) describes a *2D–3D* crossover that occurs in a certain temperature interval: when $\varepsilon << r\ \sigma_{ab}{}^{AL} \propto (\varepsilon\ r)^{-1/2}$ (*3D* mode), but at $\varepsilon >> r\ \sigma_{ab}{}^{AL} \propto \varepsilon^{-1}$ (*2D* mode). According to the theory [12], the *2D–3D* crossover should happen when

$$T_0 = T_c\{1 + 2[\xi_c(0)/d]^2\}, \quad (4)$$

where it is assumed that $\alpha = 1/2$, i.e., the following:

$$\xi_c(0) = (d/2)\varepsilon_0{}^{1/2}. \quad (5)$$

Having determined the value of ε_0 and applying the literature data on the dependence of T_c and interplanar spacing on δ [31], it was feasible to calculate the value $\xi_c(0)$.

In Figure 5 are shown the $\Delta\sigma_{ab}(T)$ dependencies in $\ln\Delta\sigma(\ln\varepsilon)$ coordinates for different r values, experimentally derived from the following relation:

$$\Delta\sigma_{abexp}(T) = 1/\rho_{exp}(T) - 1/\rho_{nab}(T), \quad (6)$$

before and after irradiation. With a temperature range between T_c and $\leq 1.1T_c$ (depending upon the oxygen concentration), these dependencies were adequately approximated by straight lines with a slope angle of $\alpha_1 \approx -0.5$, thus indicating a three-dimensional character of fluctuation superconductivity in this temperature regime. by increasing the T, the rate of decrease in Δσ increased significantly ($\alpha_2 \approx -1$). This is an indication of a change in the dimensionality of fluctuation conductivity (FC). This change corresponds to a *2D–3D* crossover. Notably, in previous studies of the FC in $YBa_2Cu_3O_{7-\delta}$ HTSC systems of various compositions using the Kouvel–Fisher method [4,6,10], a whole chain of crossovers was repeatedly recorded, and this was interpreted as a sequence of transitions of *1D–2D*, *2D–3D* and *3D*–critical fluctuations and intermediate types between them.

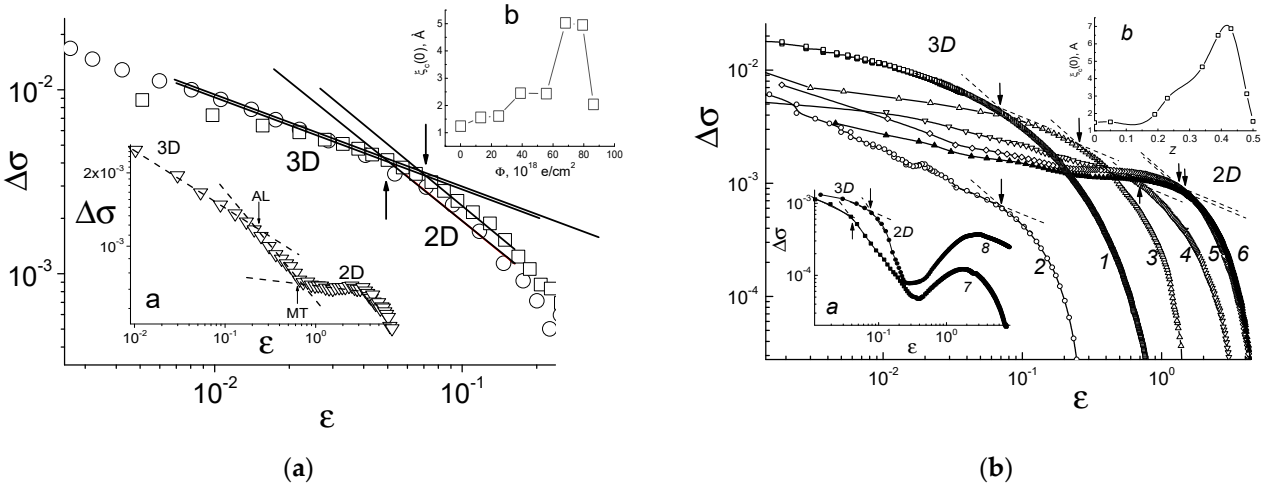

(**a**) (**b**)

Figure 5. (**a**). Dependencies $\ln\Delta\sigma(T)$ on $\ln\varepsilon$ for fluences 0 (circles) and 55.7×10^{18} e/cm^2 (squares) and 79.2×10^{18} e/cm^2 (inset (a)). The inset (b) shows the dependencies of $\xi_c(0)$ on Φ. (**b**). Temperature dependencies of excess conductivity in the *ab*-plane for $Y_{1-z}Pr_zBa_2Cu_3O_{7-\delta}$ single crystals in $\ln\Delta\sigma$-$\ln\varepsilon$ coordinates. Inset (a) shows the dependence for z = 0.48. Inset (b) shows the dependencies of $\xi_c(0)$ on z. The curves' numbering is consistent with Figure 1.

Taking into account these results, we considered the following picture of superconducting pairing in HTSC. Fluctuation pairs, nucleated inside the CuO_2 planes at $T \leq T^*$,

led to an increase in *nsc*. Since at $T >> T_c$ the values of *nsc* and especially the $\xi_c(T)$ are very small, there is likely to be no interaction between the pairs. The corresponding electronic state of the fluctuation pairs can be considered as 0-D, which is not represented by the existing FC theories. At $T \leq T_{2D}$, fluctuation pairs begin to overlap, but still only within the CuO_2 planes, forming a 2*D* electronic state, which was described by the Mackie–Thompson regime (MT) contribution of the Hikami–Larkin (HL) theory [14]. At $T \leq T_{3D}$, the increasing $\xi_c(T)$ becomes greater than *d* and connects the conducting planes by paired tunnel interactions of Josephson type. Now, the fluctuation pairs interact through the whole volume of the superconductor and form a 3*D* electronic state, which is well described by the 3*D* contribution of the Aslamazov–Larkin (AL) theory [12]. In fact, only now is the system entirely ready to complete the transition to the superconducting state.

Note that for the lnΔs(lne) dependences obtained at maximum irradiation fluences (F = 7.92 and 8.63 × 10^{19} e/cm^2), a non-monotonic progression of the curves was observed, which may have indicated an additional crossover at temperatures $e \geq e_0$ with a sharp decrease in slope, α. This behavior was already observed previously in [8] and may have indicated the possible presence of the so-called Mackie–Thompson (MT) regime of behavior of the temperature dependences of paraconductivity Δs in the system [14].

In the 2*D* region, two-particle tunneling between layers is excluded, resulting in superconducting and the normal carriers being located directly in the planes of the leading layers. The dominant contribution to the FC in this regime is made by an additional contribution, justified by Mackie–Thompson [14] and determined as a result of the interaction of the fluctuation pairs with the normal charge carriers. This contribution depends on the lifetime of fluctuation pairs and is determined by the processes of pairing for each specific sample. Importantly, the degree of heterogeneity of the sample structure has to be taken into account. According to [8], for samples of a perfect structure:

$$\sigma_{MT} = \frac{e^2}{8\hbar d(1-\alpha/\delta)} \ln\left\{\left(\frac{\delta}{\alpha}\right)\frac{1+\alpha+(1+2\alpha)^{1/2}}{1+\delta+(1+2\delta)^{1/2}}\right\}\varepsilon^{-1} \quad (7)$$

Here,

$$\alpha = 2[\xi_c(0)/d]^2\varepsilon^{-1} \text{ and } \delta = 1.203(l/\xi_{ab}(0))(16/\pi\hbar)[\xi_c(0)/d]^2 k_b T\tau_\phi \quad (8)$$

are the communication and depairing parameters, respectively. Here, *l* is the mean free path, ξ_{ab} is the coherence length in the *ab*-plane and τ_Φ is the existence time of fluctuation pairs. In the presence of inhomogeneities in the structure, the $\Delta\sigma(T)$ dependence is determined by the Lawrence–Doniach (LD) model [13].

The dependence of the coherence length $\xi_c(0)$ on the fluence of electron irradiation is shown in the inset (b) in Figure 5a.

On the main panels and inserts (a) in Figure 5a,b shows the dependencies of excess conductivity in the *ab*-plane in lnΔσ-lnε coordinates for $YBa_2Cu_3O_{7-\delta}$ (Figure 5a and insert (a)) and for $Y_{1-z}Pr_zBa_2Cu_3O_{7-\delta}$ (Figure 5b and insert (a)). The dotted lines show the approximation of the experimental curves by straight lines with slopes $\alpha_1 \approx -0.5$ (3*D* regime) and $\alpha_2 \approx -1.0$ (2*D* regime). Arrows show 2*D*–3*D* crossover points.

Insets (b) show the values of $\xi_c(0)$, calculated using Equation (5) for different Φ or *z*. It can be seen that $\xi_c(0)$ passes through a maximum at $\Phi_m \approx 80 \times 10^{18}$ e/cm^2 (Figure 5a) or $z_m \approx 0.43$ (Figure 5b).

Figure 6 shows the dependencies of $\xi_c(0)$ on T_c for all investigated samples. Dark squares show the data obtained previously for $YBa_2Cu_3O_{7-\delta}$ film samples at different volumes of δ [8]. As is known from the general theory of superconductivity (Bogoliubov–de Gennes—BdG [32]), the relationship between $\xi_c(0)$ and T_c in superconducting compounds obeys the following relation:

$$\xi_0 \sim \hbar v_F/[\pi\Delta(0)], \quad (9)$$

where $\Delta(0)$ is the order parameter at $T = 0$ K. Since for $YBa_2Cu_3O_{7-\delta}$ the value $2\Delta(0)/k_BT_c \approx 5$, then, taking $\xi_0 = \xi_c(0)$, this can be written as

$$\xi_c(0) = G/T_c \quad (10)$$

where $G = 2K\hbar v_F/(5\pi k_B)$ and the proportionality coefficient is $K \approx 0.12$.

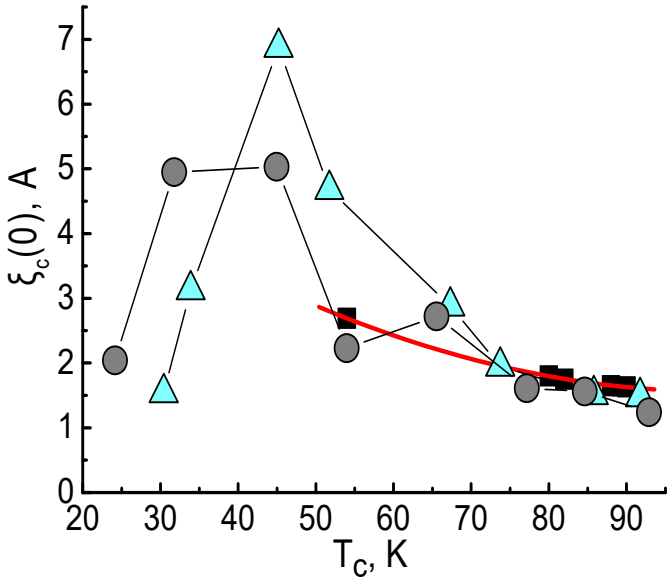

Figure 6. Dependencies of $\xi_c(0)$ on T_c for $YBa_2Cu_3O_{7-\delta}$ (circles) and for $Y_{1-z}Pr_zBa_2Cu_3O_{7-\delta}$ (triangles). Squares—data [8] for $YBa_2Cu_3O_{7-\delta}$ films.

The dependence $\xi_c(0)$ as a function of T_c is shown in Figure 6 with the red solid line, which indicates that the pairing mechanisms in HTSC films, in this range of temperatures and praseodymium concentrations, obey to a large degree the general theory of superconductivity. Qualitatively similar behavior of analogous dependencies was observed for $YBa_2Cu_3O_{7-\delta}$ (circles) and $Y_{1-z}Pr_zBa_2Cu_3O_{7-\delta}$ (triangles) single-crystal samples at $T_c \geq 65$ K and 55 K, respectively. Note that for the $\ln\Delta\sigma(\ln\varepsilon)$ dependences obtained at maximum irradiation fluences ($\surd$ = 7.92 and 8.63 $\times$ 10^{19} e/cm^2), a non-monotonic progression of the curves was observed, which may have indicated an additional crossover at temperatures $\varepsilon \geq \varepsilon_0$ with a sharp decrease in the slope, α. This behavior was already observed previously in [8] and may indicate the possible presence of the so-called Mackie–Thompson (MT) regime of behavior of the temperature dependences of paraconductivity $\Delta\sigma$ in a system [14]. Structural and kinematic anisotropy in the system can play a particular role [33–59].

4. Conclusions

The presented data and their analysis allowed us to draw a general conclusion that for optimally oxygen-doped $YBa_2Cu_3O_{7-\delta}$ single crystals, irradiation with medium fluences of high-energy electrons or an increase in the degree of doping with praseodymium leads to similar changes in the temperature dependences of electrical resistivity, ρ(T), in the ab plane. In particular, there is a significant expansion of the temperature interval of excess conductivity $\Delta\sigma(T)$ existence. In both cases, there is a multiple increase in the transverse coherence length $\xi_c(0)$ and the 2*D*–3*D* crossover point significantly shifts by temperature. It was for the first time established that, in contrast to the case of irradiation with small fluences of high-energy electrons ($\Phi \leq 10^{19}$ cm^{-2}) or with praseodymium doping to concentrations $z \leq 0.39$, irradiation with medium fluences or praseodymium doping at higher concentrations leads to a non-monotonic dependence of the transverse coherence length $\xi_c(0)$ from the critical temperature T_c, with characteristic maxima at

$\Phi \sim (7–8) \times 10^{19}$ e/cm^{-2} or $z \approx 0.42$, which may be associated with a suppression of superconducting characteristics.

Author Contributions: Conceptualization, R.V.; methodology, G.K. and A.F.; software, G.K.; formal analysis, G.K.; resources, A.F.; writing—original draft preparation, R.V. and G.K.; writing—review and editing, R.V., G.K., A.C. and I.G.; supervision, A.F. All authors have read and agreed to the published version of the manuscript.

Funding: This research received no external funding.

Institutional Review Board Statement: Not applicable.

Informed Consent Statement: Not applicable.

Data Availability Statement: The original contributions presented in the study are included in the article, further inquiries can be directed to the corresponding author.

Acknowledgments: An open access fee was paid for by the Imperial College London Open Access Fund.

Conflicts of Interest: The authors declare no conflicts of interest.

References

1. Vovk, R.V.; Solovyov, A.L. Electric transport and the pseudogap in the 1-2-3 HTSC system, under all-around compression (Review Article). *Low Temp. Phys.* **2018**, *44*, 111–153. [CrossRef]
2. Friedman, T.A.; Rice, J.P.; Giapintzakis, J.; Ginzberg, D.M. In-plane paraconductivity in a single crystal of superconducting $YBa_2Cu_3O_{7-x}$. *Phys. Rev. B* **1989**, *39*, 4258–4266. [CrossRef]
3. Jorgensen, D.; Pes, S.; Lightfoot, P.; Shi, H.; Paulikas, A.P.; Veal, B.W. Time-dependent structural phenomena at room temperature in quenched $YBa_2Cu_3O_{6.41}$: Local oxygen ordering and superconductivity. *Phys. C* **1990**, *17*, 571–578. [CrossRef]
4. Mendonca Ferreira, L.; Pureur, P.; Borges, H.A.; Lejay, P. Effects of pressure on the fluctuation conductivity of $YBa_2Cu_3O_7$. *Phys. Rev. B* **2004**, *69*, 212505. [CrossRef]
5. Petrusenko, Y.T.; Neklyudov, I.M.; Sleptsov, A.N.; Yakovlev, V.F.; Bondarenko, A.V.; Obolensky, M.A. Recovery processes in $YBa_2Cu_3O_{7-x}$ single crystals after low-temperature irradiation. *Phys. B Condens. Matter* **1991**, *169*, 711–712. [CrossRef]
6. Borges, H.A.; Continentino, M.A. Pressure study of the paraconductivity of high T_c superconductors. *Solid State Commun.* **1991**, *80*, 197–199. [CrossRef]
7. Solovjov, A.L.; Omelchenko, L.V.; Vovk, R.V.; Dobrovolskiy, O.V.; Kamchatnaya, S.N.; Sergeyev, D.M. Peculiarities in the pseudogap behavior in optimally doped $YBa_2Cu_3O_{7-\delta}$ single crystals under pressure up to 1 GPa. *Curr. Appl. Phys.* **2016**, *16*, 931–938. [CrossRef]
8. Solovjov, A.L.; Habermeier, H.-U.; Haage, T. Fluctuation conductivity in YBa2Cu3O$_{7-y}$ films with different oxygen content. I. Optimally and lightly doped YBCO films. *Low Temp. Phys.* **2002**, *28*, 17–24. [CrossRef]
9. Vovk, R.V.; Vovk, N.R.; Khadzhai, G.Y.; Goulatis, I.L.; Chroneos, A. Effect of high pressure on the electrical resistivity of optimally doped $YBa_2Cu_3O_{7-\delta}$ single crystals with unidirectional planar defects. *Phys. B Condes. Matter* **2013**, *422*, 33–35. [CrossRef]
10. Pan, V.M.; Svechnikov, V.L.; Solovjov, V.F. $YBa_2Cu_3O_{7-\text{delta}}$ single-crystal microstructure related to transport critical current density. *Supercond. Sci. Technol.* **1992**, *5*, 707. [CrossRef]
11. Timusk, T.; Statt, B. The pseudogap in high-temperature superconductors: An experimental survey. *Rep. Prog. Phys.* **1999**, *62*, 61–122. [CrossRef]
12. Aslamazov, L.G.; Larkin, A.I. The influence of fluctuation pairing of electrons on the conductivity of normal metal. *Phys. Lett. A* **1968**, *26*, 238–239. [CrossRef]
13. Lawrence, W.E.; Doniach, S. Theory of layer-structure superconductors. In Proceedings of the 12th International Conference on Low Temperature Physics, Kyoto, Japan, 4–10 September 1970; Kanda, E., Ed.; Keigaku: Tokyo, Japan, 1970; p. 361.
14. Bieri, J.B.; Maki, K.; Thompson, R.S. Nonlocal effect in magnetoconductivity of high-Tc superconductors. *Phys. Rev. B* **1991**, *44*, 4709–4711. [CrossRef] [PubMed]
15. Vovk, R.V.; Obolenskii, M.A.; Zavgorodniy, A.A.; Goulatis, I.L.; Chroneos, A.; Biletskiy, E.V. Resistive investigation of pseudogap state in non-stoichiometric $ReBa_2Cu_3O_{7-\delta}$ (Re = Y, Ho) single crystals with account for BCS–BEC crossover. *J. Alloys Compd.* **2009**, *485*, L21–L23. [CrossRef]
16. Siegrist, T.; Sunshince, S.; Murphy, D.W.; Cava, R.J.; Zahurak, S.M. Crystal structure of the high-*Tc* superconductor $Ba_2YCu_3O_{9-\delta}$. *Phys. Rev. B* **1987**, *35*, 7137–7139. [CrossRef] [PubMed]
17. Bondarenko, A.V.; Prodan, A.A.; Petrusenko, Y.T.; Borisenko, V.N.; Dworschak, F.; Dedek, U. Effect of electron irradiation on vortex dynamics in $YBa_2Cu_3O_{7-\delta}$ single crystals. *Phys. Rev. B* **2001**, *64*, 092513. [CrossRef]
18. Akhavan, M. The question of Pr in HTSC. *Phys. B Condes. Matter* **2002**, *321*, 265–282. [CrossRef]
19. Solovjov, A.L.; Omelchenko, L.V.; Petrenko, E.V.; Vovk, R.V.; Khotkevych, V.V.; Chroneos, A. Peculiarities of pseudogap in $Y_{0.95}Pr_{0.05}Ba_2Cu_3O_{7-\delta}$ single crystals under pressure up to 1.7 GPa. *Sci. Rep.* **2019**, *9*, 20424. [CrossRef]

20. Frishherz, M.C.; Kirk, M.A.; Zhang, G.P.; Weber, H.W. Transmission electron microscopy of defect cascades in $YBa_2Cu_3O_{7-\delta}$ produced by ion irradiation. *Philos. Mag. A* **1993**, *67*, 1347–1363. [CrossRef]
21. Ashkenazi, J. A Theory for the High-T_c Cuprates: Anomalous Normal-State and Spectroscopic Properties, Phase Diagram, and Pairing. *J. Supercond. Nov. Magn.* **2011**, *24*, 1281–1308. [CrossRef]
22. Vovk, R.V.; Vovk, N.R.; Shekhovtsov, O.V.; Goulatis, I.L.; Chroneos, A. *c*-axis hopping conductivity in heavily Pr-doped YBCO single crystals. *Supercond. Sci. Technol.* **2013**, *26*, 085017. [CrossRef]
23. Oduleye, O.O.; Penn, S.J.; Alford, N.M.; Lay, L.L.; Beales, T. Thermal cycling, critical current vs. strain, and finite element modelling of 1, 7, 19 and 37 filament Ag/Bi-Sr-Ca-Cu-O (BSCCO) tapes. *IEEE Trans. Appl. Supercond.* **1999**, *9*, 2621–2624. [CrossRef]
24. Wang, Q.; Saunders, G.A.; Liu, H.J.; Acres, M.S.; Almond, D.P. Electrical resistance under pressure in textured $Bi_2Sr_2CaCu_2O_{8+y}$: Enhancement of the energy gap and thermodynamic fluctuations. *Phys. Rev. B* **1997**, *55*, 8529–8543. [CrossRef]
25. Chroneos, A.I.; Goulatis, I.L.; Vovk, R.V. Atomic Scale Models for $RBa_2Cu_3O_{6.5}$ and $R_{1-X}Pr_XBa_2Cu_3O_{6.5}$ Compounds (R=Y and Lanthanides). *Acta Chim. Slov.* **2007**, *54*, 179–184.
26. Chroneos, A.; Kolesnikov, D.D.; Taranova, I.A.; Matsepulin, A.V.; Vovk, R.V. Composition variation and electron irradiation effects on the fluctuation conductivity in $Y_{1-z}Pr_zBa_2Cu_3O_{7-\delta}$ single crystals. *J. Mater. Sci. Mater. Electron.* **2020**, *31*, 19429–19436. [CrossRef]
27. Khadzhai, G.Y.; Sklyar, V.V.; Vovk, R.V. Suppression of superconductivity in $YBa_2Cu_3O_{7-\delta}$ single crystals upon irradiation with fast electrons. *Low Temp. Phys.* **2022**, *48*, 271–273. [CrossRef]
28. Anderson, P.W.; Zou, Z. "Normal" Tunneling and "Normal" Transport: Diagnostics for the Resonating-Valence-Bond State. *Phys. Rev. Lett.* **1988**, *60*, 132–135. [CrossRef]
29. Stojkovic, B.P.; Pines, D. Theory of the longitudinal and Hall conductivities of the cuprate superconductors. *Phys. Rev. B* **1997**, *55*, 8576–8595. [CrossRef]
30. Valles, J.M., Jr.; White, A.E.; Short, K.T.; Dynes, R.C.; Garno, J.P.; Levi, A.F.J.; Anzlowar, M.; Baldwin, K. Ion-beam-induced metal-insulator transition in $YBa_2Cu_3O_{7-\delta}$: A mobility edge. *Phys. Rev. B* **1989**, *39*, 11599–11602. [CrossRef] [PubMed]
31. Chryssikos, G.D.; Kamitsos, E.I.; Kapoutsis, J.A.; Patsis, A.P.; Psycharis, V.; Koufoudakis, A.; Mitros, C.; Kallias, G.; Gamari-Seale, E.; Niarchos, D. X-ray diffraction and infrared investigation of $RBa_2Cu_3O_7$ and $R_{0.5}Pr_{0.5}Ba_2Cu_3O_7$ compounds (R Y and lanthanides). *Phys. C Supercond.* **1995**, *254*, 44–62. [CrossRef]
32. De Gennes, P.G. *Superconductivity of Metals and Alloys*; W.A. Benjamin, Inc.: New York, NY, USA; Amsterdam, The Netherlands, 1966.
33. Matthews, A.J.; Kavokin, K.V.; Usher, A.; Portnoi, M.E.; Zhu, M.; Gething, J.D.; Elliot, M.; Herrenden-Harker, W.G.; Phillips, K.; Ritchie, D.A.; et al. Temperature dependence of the breakdown of the quantum Hall effect studied by induced currents. *Phys. Rev. B* **2004**, *70*, 075317. [CrossRef]
34. Adamenko, I.N.; Nemchenko, K.E.; Tsyganok, V.I.; Chervanev, A.I. Interaction of quasiparticles and stationary states of superfluid solutions of helium isotopes. *Low Temp. Phys.* **1994**, *20*, 498–504.
35. Curran, P.G.; Khotkevych, V.V.; Bending, S.J.; Gibbs, A.S.; Lee, S.L.; Mackenzie, A.P. Vortex imaging and vortex lattice transitions in superconducting Sr_2RuO_4 single crystals. *Phys. Rev. B* **2011**, *84*, 104507. [CrossRef]
36. Randeria, M. Pre-pairing for condensation. *Nat. Phys.* **2010**, *6*, 561–562. [CrossRef]
37. Badoux, S.; Tabis, W.; Laliberte, F.; Grissonnanche, G.; Vignolle, B.; Vignolles, D.; Beard, J.; Bonn, D.A.; Hardy, W.N.; Liang, R.; et al. Change of carrier density at the pseudogap critical point of a cuprate superconductor. *Nature* **2016**, *531*, 210–214. [CrossRef] [PubMed]
38. Kordyuk, A.A. Pseudogap from ARPES experiment: Three gaps in cuprates and topological superconductivity (Review Article). *Low Temp. Phys.* **2015**, *41*, 319–341. [CrossRef]
39. Solovjov, A.L. Chapter 7: Pseudogap and local pairs in high-Tc superconductors. In *Superconductors—Materials, Properties and Applications*; Gabovich, A.M., Ed.; InTech: Rijeka, Croatia, 2012; pp. 137–170.
40. He, R.-H.; Hashimoto, M.; Karapetyan, H.; Koralek, J.D.; Hinton, J.P.; Testaud, J.P.; Nathan, V.; Yoshida, Y.; Yao, H.; Tanaka, K.; et al. From a Single-Band Metal to a High-Temperature Superconductor via Two Thermal Phase Transitions. *Science* **2011**, *331*, 1579–1583. [CrossRef] [PubMed]
41. Anderson, P.W. *The Theory of Superconductivity in the High Cuprates*; Princeton University Press: Princeton, NJ, USA, 1997; p. 446.
42. Emery, V.J.; Kivelson, S.A. Importance of phase fluctuations in superconductors with small superfluid density. *Nature* **1995**, *374*, 434–437. [CrossRef]
43. Corson, J.; Mallozzi, R.; Orenstein, J.; Eckstein, J.N.; Bozovic, I. Vanishing of phase coherence in underdoped $Bi_2Sr_2CaCu_2O_{8+\delta}$. *Nature* **1999**, *398*, 221–223. [CrossRef]
44. Varma, C.M. Theory of the pseudogap state of the cuprates. *Phys. Rev. B* **2006**, *73*, 155113. [CrossRef]
45. Cava, R.J. Structural Chemistry and the Local Charge Picture of Copper Oxide Superconductors. *Science* **1990**, *247*, 656–662. [CrossRef] [PubMed]
46. Chen, Q.; Kosztin, I.; Janko, B.; Levin, K. Pairing Fluctuation Theory of Superconducting Properties in Underdoped to Overdoped Cuprates. *Phys. Rev. Lett.* **1998**, *81*, 4708–4711. [CrossRef]
47. Efetov, K.; Meier, H.; Pépin, C. Pseudogap state near a quantum critical point. *Nat. Phys.* **2013**, *9*, 442–446. [CrossRef]
48. Imada, M.; Fujimori, A.; Tokura, Y. Metal-insulator transitions. *Rev. Mod. Phys.* **1998**, *70*, 1039. [CrossRef]

49. Suzuki, M.; Watanabe, T. Discriminating the Superconducting Gap from the Pseudogap in $Bi_2Sr_2CaCu_2O_{8+\delta}$ by Interlayer Tunneling Spectroscopy. *Phys. Rev. Lett.* **2000**, *85*, 4787–4790. [CrossRef] [PubMed]
50. Habermeier, H.-U. In Proceedings of the ESF International Workshop on Superconductivity in Reduced Dimensions, Sulzburg, Austria, May 2010; p. 33.
51. Birgineau, R.J.; Shirane, G. Neutron Scattering Studies of Structural and Magnetic Excitations in Lamellar Copper Oxides. A Review. In *Physical Properties of High Temperature Superconductors I*; Ginsberg, D.M., Ed.; World Scientific: Singapore, 1989; pp. 152–212.
52. Gawalek, W.; Schueppel, W.; Hergt, R.; Andra, W.; Fischer, K.; Gornert, P. High critical currents in peritectically grown $YBa_2Cu_3O_{7-x}$ single crystals. *Supercond. Sci. Technol.* **1992**, *5*, S407–S410. [CrossRef]
53. Ando, Y.; Komiya, S.; Segawa, K.; Ono, S.; Kurita, Y. Electronic Phase Diagram of High-*Tc* Cuprate Superconductors from a Mapping of the In-Plane Resistivity Curvature. *Phys. Rev. Lett.* **2004**, *93*, 267001. [CrossRef]
54. Fehrenbacher, R.; Rice, T.M. Unusual electronic structure of $PrBa_2Cu_3O_7$. *Phys. Rev. Lett.* **1993**, *70*, 3471–3474. [CrossRef]
55. Liechtenstein, A.I.; Mazin, I.I. Quantitative model for the superconductivity suppression in R1-xPrx$Ba_2Cu_3O_7$ with different rare earths. *Phys. Rev. Lett.* **1995**, *74*, 1000–1003. [CrossRef]
56. Chu, C.W.; Hor, P.H.; Meng, R.L.; Gao, L.; Huang, A.J.; Wang, Y.Q. Evidence for superconductivity above 40 K in the La-Ba-Cu-O compound system. *Phys. Rev. Lett.* **1988**, *58*, 405–407. [CrossRef]
57. Loktev, V.M. Particularities of Superconductivity in 2D Metals: Transition from Cooper Pairing to the Local One. *Low Temp. Phys.* **1996**, *22*, 488–491.
58. Gusynin, P.; Loktev, V.M.; Sharapov, S.G. Phase diagram of a 2D metal system with a variable number of carriers. *Sov. ZETF Let.* **1997**, *65*, 182. [CrossRef]
59. Kondo, T.; Hamaya, Y.; Palczewski, A.D.; Takeuchi, T.; Wen, J.S.; Xu, Z.J.; Gu, G.; Schmalian, J.; Kaminski, A. Disentangling Cooper-pair formation above the transition temperature from the pseudogap state in the cuprates. *Nat. Phys.* **2011**, *7*, 21–25. [CrossRef]